

The influence of star formation history on the gravitational wave signal from close double degenerates in the thin disc

Shenghua Yu and C. Simon Jeffery
Armagh Observatory, College Hill, Armagh BT61 9DG, N. Ireland

Accepted . Received ;

ABSTRACT

The expected gravitational wave (GW) signal due to double degenerates (DDs) in the thin Galactic disc is calculated using a Monte Carlo simulation. The number of young close DDs that will contribute observable discrete signals in the frequency range 1.58–15.8 mHz is estimated by comparison with the sensitivity of proposed GW observatories. The present-day DD population is examined as a function of Galactic star-formation history alone. It is shown that the frequency distribution, in particular, is a sensitive function of the Galactic star formation history and could be used to measure the time since the last major star-formation epoch.

Key words: stars: white dwarfs – stars: evolution – stars: binaries: close – stars: formation – Galaxy: evolution – Galaxy: structure

1 INTRODUCTION

Theoretical studies have indicated that double degenerate (DD) stars with very close orbital separation should be the most abundant and prominent sources of gravitational wave (GW) radiation at frequencies between 0.1 and 30 mHz (Peters & Mathews 1963; Landau & Lifshitz 1975; Evans et al. 1987). In addition to other binaries, they will form a GW confusion background due to the large number of sources per frequency resolution bin (Hils et al. 1990; Hils & Bender 2000).

In general, the number of DDs per equal-interval frequency bin at high frequency in any Galactic population drops as a function of frequency. For a frequency resolution better than $\sim 3 \times 10^{-8}$ Hz and frequencies $\gtrsim 1$ mHz (i.e. orbital periods ≤ 33 min), a GW experiment may detect only one or no individual sources per resolution bin, making the source potentially resolvable¹ (Evans et al. 1987; Hils & Bender 2000; Nelemans et al. 2001; Ruiter et al. 2009; Yu & Jeffery 2010). Resolved DDs identified from GW detections would allow us to study the relation between their properties and the dynamic nature of globular clusters (Willems et al. 2007), the nature and potential outcome of the DD merging process (Webbink 1984),

and their association with the formation and evolution of a galaxy.

Since DDs in a galaxy are the outcome of stellar formation and evolution, a key question is how the star formation (SF) history, the distribution of initial orbital parameters and the evolution of their main-sequence progenitors influence the DD population in terms of final distribution with orbital period (GW frequency), separation and chirp mass². This question can be addressed using the method of binary-star population synthesis (BSPS) to investigate, for example, the SF history alone. In our previous papers (Yu & Jeffery 2010, 2011), the influence of star formation and evolution on the DDs in a galaxy was characterised by the use of a parameteric SF rate and synthetic SF contribution functions.

The SF history in a galaxy is likely to be more complicated than approximations used in previous studies, for example, a single star-burst, constant SF, or (quasi-) exponential SF (Nelemans et al. (2001); Ruiter et al. (2009); Yu & Jeffery (2010)). Observations agree that the SF rate in the Galactic disc is likely to be declining but is episodically enhanced (Majewski 1993; Rocha-Pinto et al. 2000). The aim of this paper is to show how the GW signal from

¹ If there is only one DD in a resolution bin and the GW signal from this DD is greater than a given detection threshold (e.g. S/N=3 in this paper), we define the DD to be a resolved source. If the GW signal from this DD is less than the same detection threshold (e.g. S/N=3 in this paper), we define the DD to be a potentially resolved source.

² Chirp mass (\mathcal{M}) of a binary is defined as $\mathcal{M} \equiv \left(\frac{m_1 m_2}{m_1 + m_2}\right)^{3/5} (m_1 + m_2)^{2/5}$ where m_1 and m_2 is the mass of each component of the binary respectively. A general relation between the GW frequency f and the orbital period P_{orb} in the n th harmonic is $f = \frac{n}{P_{\text{orb}}}$. In particular, if a binary is in a circular orbit (eccentricity $e=0$), we have $f = \frac{2}{P_{\text{orb}}}$.

the DD population in the thin disc in the Galaxy depends on the SF history whilst keeping other factors in the model constant.

We compute the GW signal from a simulated DD population in the thin disc of the Galaxy in § 2, and compare the results for three different SF models in § 3. We compare our results with previous studies in § 4, and draw significant conclusions in § 5.

2 THE GW SIGNAL FROM RESOLVED DOUBLE DEGENERATES IN THE THIN DISC

We simulate the DD population in the thin disc of the Galaxy by adopting a simplified binary-star evolution and population-synthesis model (BSPS). Inputs include a star formation rate (SFR), an initial mass function (IMF), a mass ratio distribution P_q , an orbital separation distribution P_a , an eccentricity distribution P_e , a metallicity Z and a representation of the thin disc structure (Yu & Jeffery 2010). If the orbital period of a binary is sufficiently long (i.e. $\gtrsim 100$ yrs), the binary is assumed to behave as two single stars and will not form a DD. Inputs also include binary-star evolution physics, including mass-loss rates, common-envelope ejection efficiency, etc., described by Yu & Jeffery (2010).

To provide a benchmark calculation, the SFR is approximated by a quasi-exponential function

$$S(t) = 7.92e^{-t/\tau} + 0.09t \text{ M}_\odot \text{yr}^{-1} \quad (1)$$

where t is the age of the disc and $\tau = 9$ Gyr, yielding an SFR $\approx 3.5 \text{M}_\odot \text{yr}^{-1}$ and a total disc mass (in stars) $M_d \approx 5.2 \times 10^{10} \text{M}_\odot$ at the current epoch ($t = 10$ Gyr). The value for the current SFR is consistent with recent observations (Diehl et al. 2006). We adopt the IMF of Kroupa et al. (1993), a constant P_q (Mazeh et al. 1992; Goldberg & Mazeh 1994), and P_a following Han (1998) and Griffin (1985). $P_e = 2e$ follows Nelemans et al. (2001). We adopt $Z = 0.02$ (solar) for all thin disc binaries.

The simulation is started with a sample of 10^7 primordial MS+MS binaries, with total mass $\approx 1.05 \times 10^7 \text{M}_\odot$. Initial parameters for each binary are allocated on the above distributions using a Monte Carlo procedure. This procedure yields a total of $\sim 4.93 \times 10^4$ DDs over a period of 15 Gyr. We compute the birth rate, merger rate and total number, and record their individual properties (masses and orbital parameters) as a function of the age of the thin disc (Yu & Jeffery 2011).

Subsequently, a second Monte Carlo procedure is used to generate the orbital properties for a complete sample of n_{dd} thin-disc DDs by interpolation on the initial DD sample described above. The initial DD sample obtained from computations of stellar evolution and the complete sample are identical with Yu & Jeffery (2011), and similar to Yu & Jeffery (2010) (the difference to the total number DDs in the thin disc is $\sim 8\%$). We identify four types of DD pair by the chemical composition of their degenerate cores, i.e. He+He, CO+He, CO+CO, and ONeMg+X where X = He, CO, or ONeMg. Since we use a simplified model, the criteria for identifying the WD core compositions are given by the initial-final mass relation (Han 1998; Hurley et al. 2000, 2002).

Yu & Jeffery (2011) give n_{dd} for the four different types of DD in this simulation. These n_{dd} DDs are distributed in a thin disc model where the stellar mass density is described as

$$\rho_d(R, z) = \frac{M_d}{4\pi h_R^2 h_z} e^{-R/h_R} \operatorname{sech}^2(-z/h_z) \text{ M}_\odot \text{pc}^{-3}, \quad (2)$$

and where R and z are the natural cylindrical coordinates of the axisymmetric disc, and $h_R = 2.5$ kpc and $h_z = 0.352$ kpc are the radial scale length and scale height of the thin disc (Sackett 1997; Phleps et al. 2000). This structure and the thin disc mass (in stars) are consistent with the dynamical parameters given by Klypin et al. (2002) and Robin et al. (2003).

The DDs are sorted to obtain the number distribution by orbital frequency, to calculate the total strain amplitude $\sum h^2$ from all DDs in each frequency bin, and hence to obtain the GW strain amplitude-frequency relation due to the thin disc DDs. We adopt a frequency resolution element $\Delta f = 3.17 \times 10^{-8}$ Hz, corresponding to one year of observation with a GW detector.

Figure 1 illustrates the influence from different SF epochs on the predicted GW signal. The expected sensitivities for S/N=3 for the proposed GW detectors eLISA and LAGRANGE (or eLISA-type mission) in a one year mission are also shown (Larson et al. 2000; Conklin et al. 2011).

From this figure, we identify a turning point, or critical frequency f_c , around 0.001 Hz. For frequencies $f < f_c$, the amplitude of the GW varies approximately *inversely* with frequency, forming a ‘continuum’. For frequencies above the critical frequency f_c , the amplitude becomes a discrete signal.

The existence of the critical frequency is strongly associated with the product of the number distribution of DDs with respect to the frequency and the size of the frequency element, i.e. $\frac{dn(f)}{df} \Delta f$. When $f \leq f_c$, i.e. $\frac{dn(f)}{df} \Delta f \geq 1$, there must be one or more DDs per resolution element Δf , implying that $n(f)$ can be represented by a continuous function. When $f > f_c$, i.e. $\frac{dn(f)}{df} \Delta f < 1$, some frequency bins will not contain any DD. Rather, there will be one DD in $i = (\frac{dn(f)}{df} \Delta f)^{-1}$ frequency bins, i.e. in one frequency bin between f and $f + i\Delta f$.

These results are consistent with an analytic approach (e.g. Evans et al. (1987)), whereby

$$f_c = 2.977 \left(\frac{\mathcal{M}}{M_\odot} \right)^{-5/11} \left(\frac{\nu}{\text{yr}^{-1}} \right)^{3/11} \left(\frac{\Delta f}{10^{-8}} \right)^{3/11} \text{mHz}, \quad (3)$$

in which the chirp mass \mathcal{M} of a binary is assumed to be an independent variable and $\nu \equiv \int \nu(f) df$ is the total birth rate of DDs.

Figure 1 shows that the continuum of the thin disc GW signal consists mainly of signal from early SF (i.e. 0.0 – 6.0 Gyr). Late SF (i.e. 8.0–9.95 Gyr) contributes most of the discrete signal in the high frequency band and only a small fraction of the continuum. Sources with $\log f > -2.3$ principally comprise CO+He and He+He DDs formed during the last epoch of SF. In the range $-3 < \log f < -2.3$, different types of DD will be mixed, with CO+CO and ONeMg+X DDs dominating the high amplitude signal and CO+He and He+He DDs contributing to the low amplitude. We are primarily interested in these resolved sources since their strain

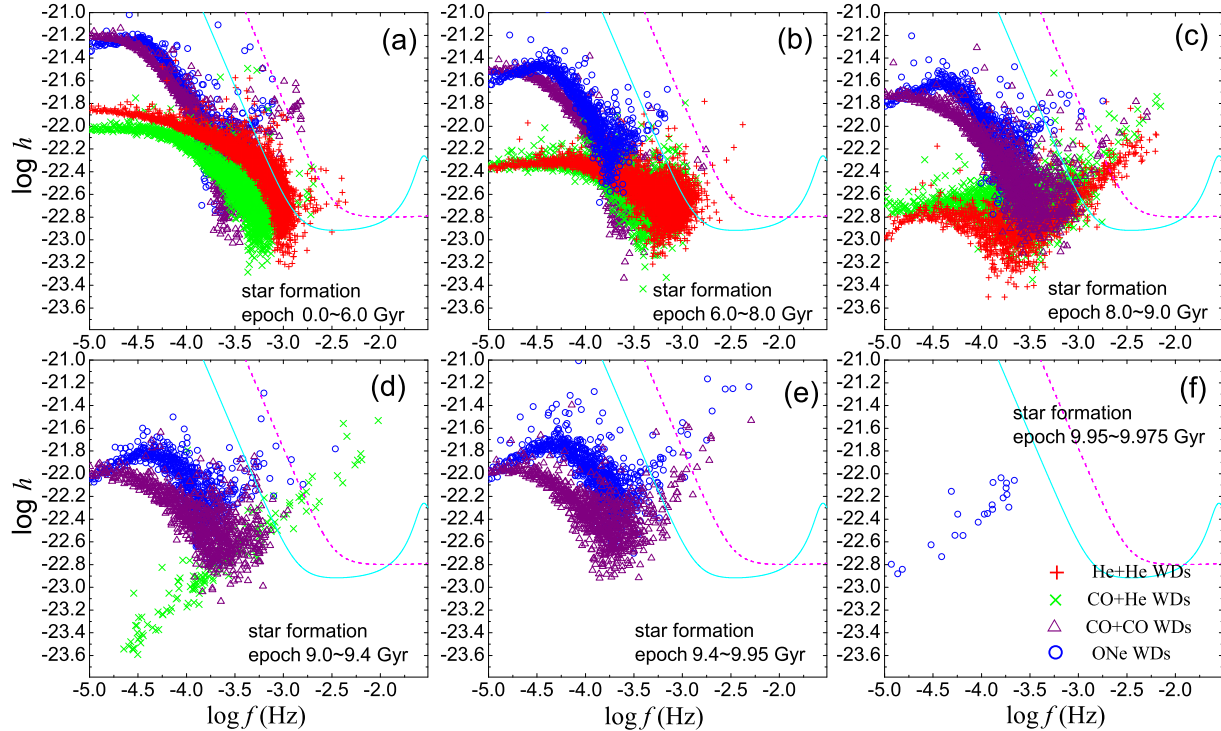


Figure 1. The contribution of the current DD populations from different star-formation epochs to the gravitational-wave amplitude ($\log h$) in the quasi-exponential star-formation model. Solid (cyan) and broken (magenta) lines represent the eLISA and LAGRANGE sensitivity with $S/N=3$ for a one year mission, respectively.

amplitudes exceed the sensitivities of the proposed GW detectors.

In addition, distance strongly affects the GW signal, both continuum and discrete. The structure of the thin disc implies that the distance to the majority of DDs will be large, but there will be a few nearby (local) DDs. Thus, in our simulations, there are few isolated strong signals due to DDs at $d < 1$ kpc (*e.g.* Fig. 1(b): $\log f = -2.88$ and $\log f = -2.98$).

3 COMPARISON OF DIFFERENT STAR FORMATION MODELS

We have discussed the GW signal with a ‘*Quasi-Exponential SF*’ rate. In order to see the influence on the GW signal from different SF models, we have calculated the GW signal assuming two further models for the SF rate. These are ‘*Instantaneous SF*’, in which a single star burst takes place only at the formation of the thin disc with a constant SF rate of $132.9 M_{\odot} \text{ yr}^{-1}$ from 0 to 391 Myr, and ‘*Constant SF*’, in which SF occurs at a constant rate of $5.2 M_{\odot} \text{ yr}^{-1}$ from 0 to 10 Gyr. All three models produce a thin-disc star mass of $\sim 5.2 \times 10^{10} M_{\odot}$ at the thin-disc age $t = 10$ Gyr.

The differences between the signals in these models arise from DDs with different progenitor properties. According to binary-star evolution theory, main sequence stars with mass

$M \leq 2M_{\odot}$ can leave low-mass white dwarfs (WDs) with core mass $\lesssim 0.5 M_{\odot}$ if there is no significant mass accretion (*e.g.* Hurley et al. (2002)). Stars with $M \approx 2 - 10 M_{\odot}$ can develop WDs with massive degenerate cores ($\gtrsim 0.5 M_{\odot}$) and heavier elements (*i.e.* CO or ONeMg). Since the evolution time-scale of a star is a strong function of its initial mass, the birth rates of different WD types and the GW signal are sensitive to different SF epochs. For example, the signals at high frequency from He+He and CO+He DDs are sensitive to SF between 6–9 and 8–9.4 Gyr respectively (Fig. 1). Our results show that a constant SF model produces a distinctly higher strain amplitude from He+He DDs ($-22.2 < \log h < -23.0$, $-2.8 < \log f < -2.0$) than both other models. The quasi-exponential model produces less high-frequency GW radiation than the constant SF model.

However, a very different discrete GW signal at $f > 0.001$ Hz is produced by the *instantaneous SF* model. The bottom panel in Fig. 2 shows only a few GW signals from close DDs at $f \gtrsim 0.00158$ Hz ($\log f \gtrsim -2.8$). Since the majority of close DDs merged in the past 10 Gyr (see birth and merger rates in Yu & Jeffery (2011)), only a few close DDs now remain. This implies that short-period DDs producing the discrete GW signal are sensitive to recent SF (see Fig. 1).

To represent possible future observations, the sensitivities of the proposed eLISA and LAGRANGE missions are shown in each figure. In our present simulations, the number of (one-year) resolvable DDs are 11880, 22920 and 16240 for

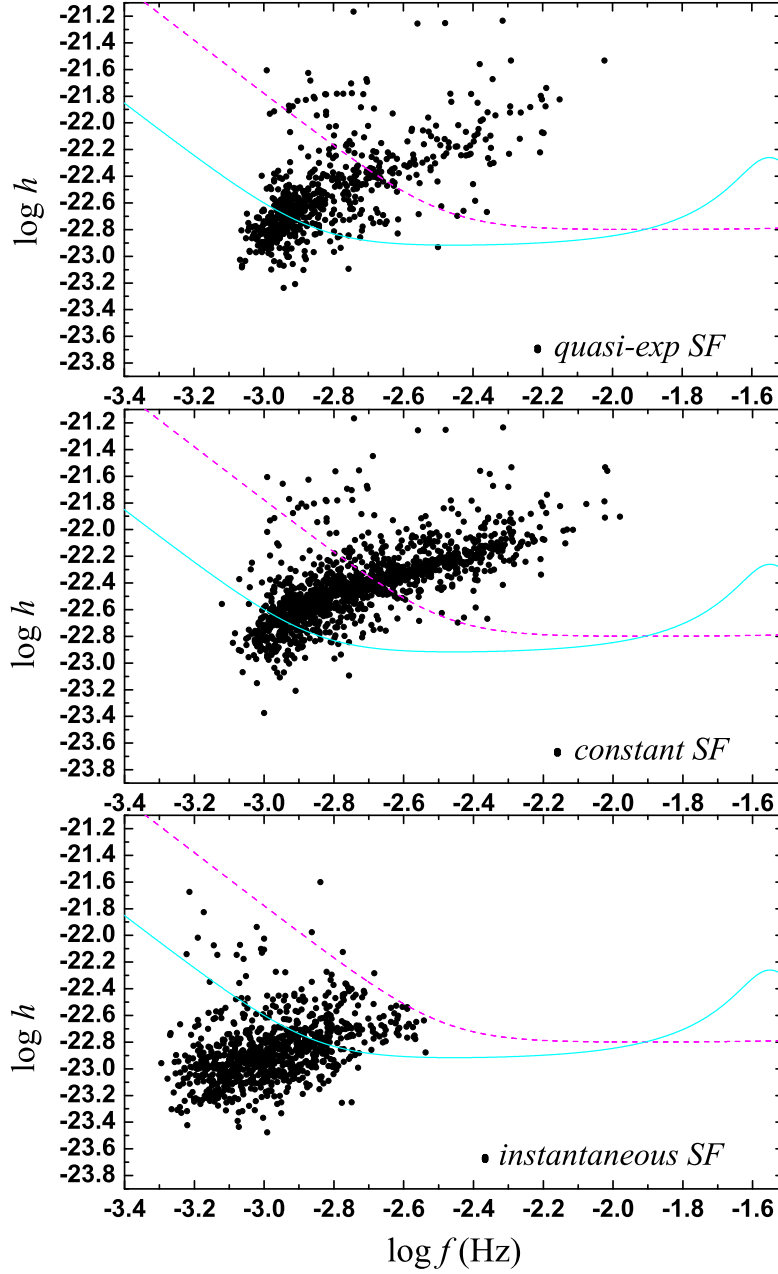


Figure 2. Resolved and potentially resolved DDs in the different star-formation models. From top to bottom, the SF models are quasi-exponential, constant and instantaneous (§ 3). Solid (cyan) and broken (magenta) lines represent the eLISA and LAGRANGE sensitivity with S/N=3 for a one year mission, respectively. For clarity, the systems shown represent a small sample (one DD in twenty) of the complete thin-disc simulations.

the quasi-exponential, constant, and instantaneous SF models respectively, in which about 2690, 9020 and 80 could be resolved by LAGRANGE with S/N=3, and about 8010, 19820, 3840 could be resolved by eLISA with S/N=3. These systems are shown in Fig. 2. The proportion of each type of DD is shown in Table 1. The proportions of resolvable DDs detectable by LAGRANGE are quite different from those

given by the models because of the frequency response of the detector. LAGRANGE is more sensitive to high- f DDs, of which the highest proportion are found in the constant SF model, which contains the highest fraction of DDs from recent star formation.

Figure 3 shows the distribution of the GW strain am-

Table 1. Proportion of each type of resolved DD in each SF model.

	quasi-exp	constant	instantaneous
types of DDs			
He+He	71.0%	78.9%	74.6%
CO+He	22.6%	16.2%	17.1%
CO+CO	5.5%	4.1%	7.8%
ONeMg+X	0.9%	0.8%	0.4%
total	11880	22920	16240
resolved by LAGRANGE with S/N=3	2690	9020	80
resolved by eLISA with S/N=3	8010	19820	3840

plitude and frequency from all resolvable DDs in each SF model. This figure can be understood analytically.

The change of orbital separation \dot{a} of a DD in a circular orbit with respect to time due to GW radiation is (Landau & Lifshitz 1975)

$$\dot{a} = -\frac{64}{5}G^3c^{-5}\mu M^2a^{-3}. \quad (4)$$

where a is the orbital separation; G is the gravitational constant; c is the speed of light; μ and M are the reduced mass and total mass of the DD, respectively. Combining Eq. 4 with Kepler's third law $P_{\text{orb}}^2/a^3 = 4\pi^2/GM$ and the relation between orbital period and GW frequency $P_{\text{orb}} = 2/\dot{f}$, we have the change of the GW frequency of a DD per unit time

$$\dot{f} = -\frac{96}{5}G^{5/3}c^{-5}\pi^{8/3}\mathcal{M}^{5/3}\dot{a}^{11/3}, \quad (5)$$

where $\mathcal{M} \equiv \mu^{3/5}M^{2/5}$ is the chirp mass (see footnote 2). The inverse \dot{f}^{-1} indicates the GW radiation timescale or lifetime.

Assuming that the birth rate of the DDs at frequency f is $\nu(f)$, the number of DDs per unit frequency may be written as the product of birth rate and lifetime; using appropriate units

$$\begin{aligned} \frac{dn(f)}{df} &= \nu(f) \cdot \dot{f}^{-1} \\ &= \frac{\nu(f)}{\frac{96}{5}G^{5/3}c^{-5}\pi^{8/3}\mathcal{M}^{5/3}\dot{a}^{11/3}} \\ &\approx 0.0546(\mathcal{M}/M_{\odot})^{-5/3}(\nu(f)/\text{yr}^{-1})(f/\text{Hz})^{-11/3} \text{ Hz}^{-1}. \end{aligned} \quad (6)$$

Hence the number distribution has contributions from the birth-rate $\nu(f)$, which is important when significant numbers of young DDs are being injected into the population at high frequencies, and from the orbital decay lifetime which gives the $f^{-11/3}$ distribution and which is important when short-period DDs have all evolved from old long-period DDs.

To illustrate, we assume that $\nu(f)$ and \mathcal{M} are independent of frequency f . If $\mathcal{M} = 0.5 M_{\odot}$ and $\nu = 0.004 \text{ yr}^{-1}$ (average values estimated from simulations with quasi-exponential SF in the frequency range $10^{-5} - 10^{-1.6} \text{ Hz}$), the number probability of DDs $\frac{dn(f)}{df} \approx 0.0007f^{-11/3}$ ($df = 1 \text{ yr}^{-1}$). This relation is plotted in Fig. 3 and has the same slope as the simulation with instantaneous SF (approximately a δ -function) for $\log f > -2.8$.

The differences between the number distributions of resolved DDs in the three SF models can be understood simply in terms of the SF history. The DD birth rate $\nu(f, t)$ can be expressed as $\nu(f, t_{\text{disc}}) = \int_0^{t_{\text{disc}}} \ddot{C}_*(f, t_{\text{disc}} - t_{\text{sf}})S(t_{\text{sf}})dt_{\text{sf}}$ where t_{disc} is the age of the thin disc, t_{sf} is the time of star formation, \ddot{C}_* is the contribution function, and S is the star formation rate. \ddot{C}_* provides information about the number and frequency distribution of DDs from a given epoch, and is independent of the SF history (see § 2.1 and Figs. 6-7 in Yu & Jeffery (2011) for details). The DD birth rate is obtained by convolution with S .

If S is a δ -function, the birth rate of DDs after 10 Gyr is a very weak function of f . Most present-day close DDs would be long-evolved DD systems, so their number distribution follows the power-law relation $f^{-11/3}$ (Fig. 3). However, if S is continuous over 10 Gyr, contributions at every SF epoch must be included and will increase the number of DDs at high frequency.

Thus, assuming that (a) all other inputs to the BSPS model are valid (or at least that systematic errors can be eliminated by other means) and (b) there is no significant contamination by resolved sources from other locations, it is evident that GW observations of DDs could distinguish between different SF histories. In particular, the frequency above which the distribution develops a $f^{-11/3}$ gradient is indicative of the time since the last major SF epoch.

4 DISCUSSION

The impact of different SF histories provides one reason for the differences between calculations of DD number distributions and GW strain amplitude-frequency relation by different authors (Evans et al. 1987; Nelemans et al. 2001; Ruiter et al. 2009; Yu & Jeffery 2010), especially where these authors adopt similar approximations for the physics of binary star evolution. The method of interpolation (see § 2) is important for predicting the absolute number of resolved DDs but not crucial for the relative numbers in different models. In the present simulation, we only interpolate to produce a complete Galactic sample from the more limited BSPS sample. There is no extrapolation and the interpolation errors decrease the predicted GW strain and the number of resolved DDs by no more than $\sim 30\%$.

Nelemans et al. (2004) estimate that there may be $\approx 2.13 \times 10^8$ close detached DDs in the Galactic bulge and disc, with $\approx 2.3 \times 10^7$ semi-detached DDs, assuming an age of 13.5

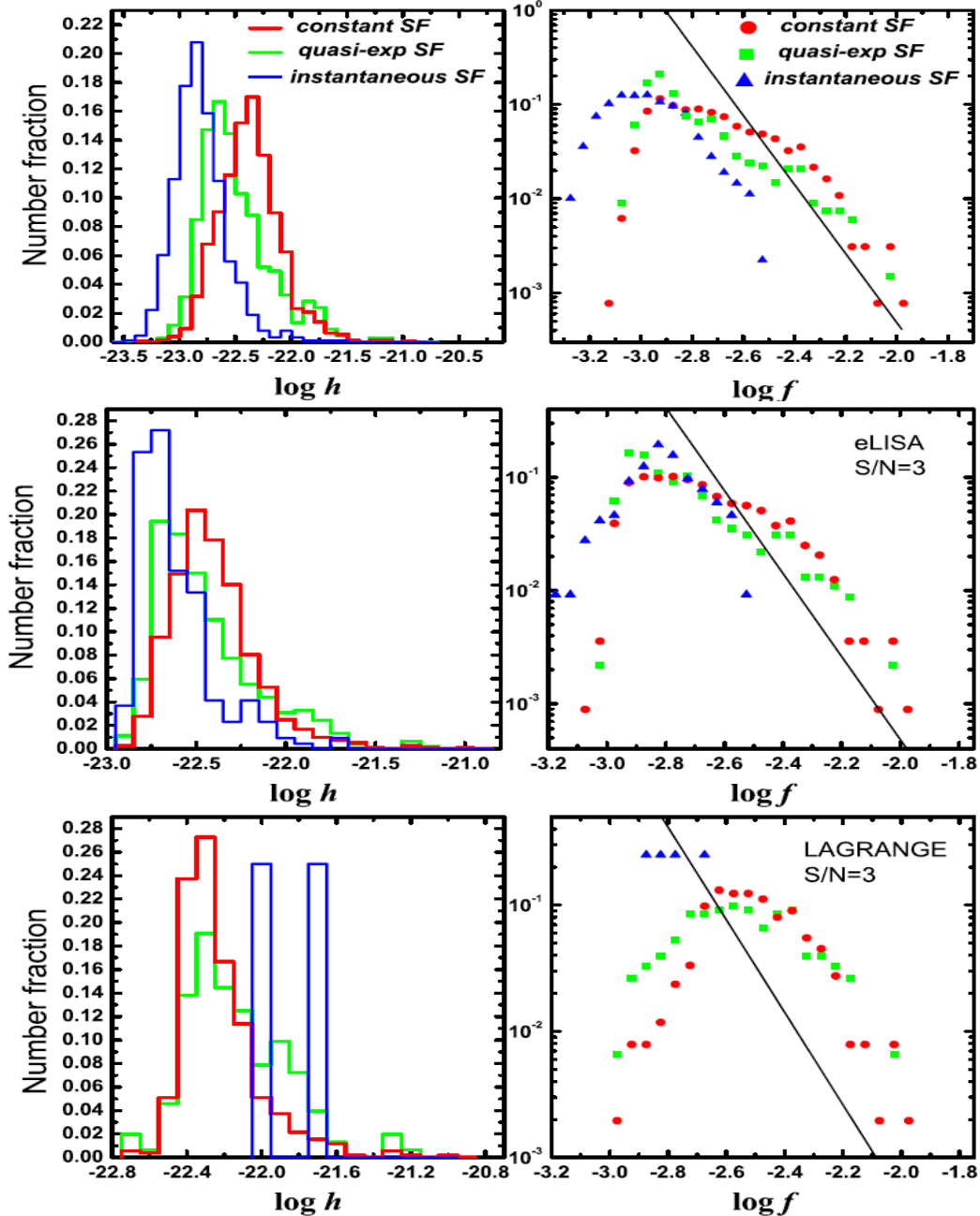


Figure 3. Histogram of the GW signal distribution from resolvable DDs, including resolved and potentially resolved DDs (top panels) and from resolved DDs by the two GW detectors (middle and bottom panels) with respect to strain amplitude (left) and frequency (right) in different SF models, with $\Delta \log h = 0.1$ and $\Delta \log f = 0.05$. Blue represents the instantaneous star formation (SF) model, red, constant SF, and green, quasi-exponential SF. The straight black line represents the number-frequency relation: $\frac{dn(f)}{df} \approx 0.0007f^{-11/3}$, $df = 1 \text{ yr}^{-1}$. Top panels: no correction for detector sensitivity, Middle: relative distributions assuming an eLISA-type detector with $S/N=3$, Bottom: relative distributions assuming a LAGRANGE-type detector with $S/N=3$. All number fractions are normalized to the total numbers of resolved DDs in each model (Table 1).

Gyr and a SF history following Boissier & Prantzos (1999). We find $\approx 2.4 \pm 0.5 \times 10^8$ DDs in the bulge and thin disc, with $\approx 5 \times 10^5$ semi-detached DDs ($\approx 0.3\%$ of all DDs in the thin disc) (Yu & Jeffery 2010, 2011). The average birth rate of DDs given by Nelemans et al. (2004) ($1.58 \times 10^{-2} \text{ yr}^{-1}$) is slightly less than our result ($2.4 \times 10^{-2} \text{ yr}^{-1}$). However, we give a much lower average birth rate for semi-detached DDs $\approx 5 \times 10^{-5} \text{ yr}^{-1}$, compared with $\approx 1.7 \times 10^{-3} \text{ yr}^{-1}$

by Nelemans et al. (2004). The local space density of semi-detached DDs in our quasi-exponential SF model of the thin disc is $\approx 6.2 \times 10^{-7} \text{ pc}^{-3}$, slightly less than the constraint of $1 - 3 \times 10^{-6} \text{ pc}^{-3}$ obtained from the Sloan Digital Sky Survey (Roelofs et al. 2007) on the assumption that semi-detached He+He and CO+He DDs look like AM Canum Venaticorum binaries.

Ruiter et al. (2010) estimate there to be $\approx 2.48 \times 10^7$ DDs with orbital periods in the range 200 s to 5.6 hr in the Galactic disc, including $\approx 1.62 \times 10^7$ semi-detached DDs ($\sim 65\%$ of all DDs). They assume a constant SF rate ($4 M_\odot \text{ yr}^{-1}$) in the disc for 10 Gyr. The average birth rate of DDs in this period range is $\sim 2.48 \times 10^{-3} \text{ yr}^{-1}$, while the average birth rate of semi-detached DDs is $\sim 1.62 \times 10^{-3} \text{ yr}^{-1}$. The latter is significantly higher than our result. The local density of semi-detached DDs in Ruiter et al. (2010), $2.3 \times 10^{-5} \text{ pc}^{-3}$, is substantially higher than both our value and the observation. The formulae adopted to simulate Galactic structure may contribute a significant fraction of the differences in estimates of the local density of DDs; Nelemans et al. (2004), Ruiter et al. (2010), and ourselves adopted density distributions $\rho \propto \text{sech}(z/h_z)^2$, $\rho \propto e^{(|-z|/h_z)}$, and $\rho \propto \text{sech}^2(-z/h_z)$ respectively, where ρ is mass density, z the height of the thin disc in the cylindrical coordinates, and h_z the scale height of the thin disc (Yu & Jeffery 2010).

Nissanke et al. (2012) recently confirmed that thousands of detached DDs may be detected by space-borne GW detectors with 5 and 1 Mkm arms, but there may be only a few ten to a few hundred detections of interacting DD systems. This is attributed to an assessment of detection prospects, based on iterative identification and subtraction of bright sources with respect to both instrument and confusion noise. Our results also imply that detached DDs will dominate the GW signal from the total Galactic DD population in the GW frequency range of $10^{-5} - 10^{-1.6} \text{ Hz}$. However, they also argue that the SF history of the disc is an important factor and may affect the number ratio of the detached and semi-detached DDs detected by a GW observatory.

Since the GW background may be affected by sources including DDs beyond the Milky Way, an estimate of contamination from the Local Group would be of interest. Observations indicate that SF history in the Local Group is complicated. For instance, the Large Magellanic Cloud (LMC) most likely experienced a dramatic decrease of SF following an initial star burst some 12 Gyr ago. SF resumed some 5 Gyr ago has since proceeded with a low average rate of roughly $0.2 M_\odot \text{ yr}^{-1}$, peaking roughly 2 Gyr, 0.5 Gyr, 0.1 Gyr and 0.012 Gyr ago (Harris & Zaritsky 2009). The Small Magellanic Cloud (SMC) has a similar history to the LMC, but with a different look-back time for the initial star burst (≈ 8.4 Gyr) and with minor star bursts roughly 2.5, 0.4, and 0.06 Gyr ago (Harris & Zaritsky 2004). Our results (e.g. Fig. 1) show that recent (2 Gyr) SF has a significant contribution to the GW signal from DDs in the Galactic thin disc. Assuming that DD contribution functions are the same for both the Galaxy and for the LMC and SMC, the GW signal from the thin-disc DDs may well be contaminated by DDs in other Local Group galaxies. This should be explored in the future.

5 CONCLUSION

Monte Carlo simulations have been carried out to synthesize the GW signal from DDs based on a binary-evolution model (Han 1998; Hurley et al. 2002; Yu & Jeffery 2010), different star-formation models and the present thin disc structure

of the Galaxy. The GW signal consists of a continuum at low frequency and a discrete signal at high frequency. The continuum arises mainly from DDs with main-sequence progenitors formed in the early disc (i.e. between 0 and 8 Gyr). Recent SF (i.e. between 8 and 10 Gyr) gives rise to a significant fraction of short-period DDs corresponding to the GW signal at high frequency, which is mostly resolved and which is thus sensitive to the recent star-formation history. At the highest frequencies, where the orbital-decay timescale governs the evolution, we have shown that our Monte Carlo simulations reproduce the distribution expected from analytic approximation. Both the intercept of the high-frequency distribution of the resolved DD population and the frequency below which the distribution drops below that predicted by the orbital-decay timescale are sensitive to recent star formation.

Since the high-frequency GW signal is dominated by DDs from recent star formation, future work should explore whether GW observations can be used to constrain the time since the most recent major burst of star formation in the Galaxy.

6 ACKNOWLEDGEMENTS

The Armagh Observatory is supported by a grant from the Northern Ireland Dept. of Culture Arts and Leisure. We thank the referee for the constructive suggestions and comments.

REFERENCES

- Boissier S., Prantzos N., 1999, MNRAS, 307, 857
- Conklin J. W., Buchman S., Aguero V. e. a., 2011, ArXiv e-prints
- Diehl R., Halloin H., Kretschmer K., Lichti G. G., Schönfelder V., Strong A. W., von Kienlin A., Wang W., Jean P., Knöldlseder J., Roques J., Weidenspointner G., Schanne S., Hartmann D. H., Winkler C., Wunderer C., 2006, Nature, 439, 45
- Evans C. R., Iben I. J., Smarr L., 1987, ApJ, 323, 129
- Goldberg D., Mazeh T., 1994, A&A, 282, 801
- Griffin R. F., 1985, in P. P. Eggleton & J. E. Pringle ed., NATO ASIC Proc. 150: Interacting Binaries The distributions of periods and amplitudes of late-type spectroscopic binaries. pp 1–12
- Han Z., 1998, MNRAS, 296, 1019
- Harris J., Zaritsky D., 2004, AJ, 127, 1531
- Harris J., Zaritsky D., 2009, AJ, 138, 1243
- Hils D., Bender P. L., 2000, ApJ, 537, 334
- Hils D., Bender P. L., Webbink R. F., 1990, ApJ, 360, 75
- Hurley J. R., Pols O. R., Tout C. A., 2000, MNRAS, 315, 543
- Hurley J. R., Tout C. A., Pols O. R., 2002, MNRAS, 329, 897
- Klypin A., Zhao H., Somerville R. S., 2002, ApJ, 573, 597
- Kroupa P., Tout C. A., Gilmore G., 1993, MNRAS, 262, 545
- Landau L. D., Lifshitz E. M., 1975, The classical theory of fields. Course of theoretical physics - Pergamon International Library of Science, Technology, Engineering

- and Social Studies, Oxford: Pergamon Press, 1975, 4th rev.engl.ed.
- Larson S. L., Hiscock W. A., Hellings R. W., 2000, Phys. Rev. D, 62, 062001
- Majewski S. R., 1993, ARA&A, 31, 575
- Mazeh T., Goldberg D., Duquennoy A., Mayor M., 1992, ApJ, 401, 265
- Nelemans G., Yungelson L. R., Portegies Zwart S. F., 2001, A&A, 375, 890
- Nelemans G., Yungelson L. R., Portegies Zwart S. F., 2004, MNRAS, 349, 181
- Nissanke S., Vallisneri M., Nelemans G., Prince T. A., 2012, ApJ, 758, 131
- Peters P. C., Mathews J., 1963, Physical Review, 131, 435
- Phleps S., Meisenheimer K., Fuchs B., Wolf C., 2000, A&A, 356, 108
- Robin A. C., Reylé C., Derrière S., Picaud S., 2003, A&A, 409, 523
- Rocha-Pinto H. J., Scalo J., Maciel W. J., Flynn C., 2000, A&A, 358, 869
- Roelofs G. H. A., Groot P. J., Benedict G. F., McArthur B. E., Steeghs D., Morales-Rueda L., Marsh T. R., Nelemans G., 2007, ApJ, 666, 1174
- Ruiter A. J., Belczynski K., Benacquista M., Holley-Bockelmann K., 2009, ApJ, 693, 383
- Ruiter A. J., Belczynski K., Benacquista M., Larson S. L., Williams G., 2010, ApJ, 717, 1006
- Sackett P. D., 1997, ApJ, 483, 103
- Webbink R. F., 1984, ApJ, 277, 355
- Willems B., Kalogera V., Vecchio A., Ivanova N., Rasio F. A., Fregeau J. M., Belczynski K., 2007, ApJ, 665, L59
- Yu S., Jeffery C. S., 2010, A&A, 521, A85+
- Yu S., Jeffery C. S., 2011, MNRAS, 417, 1392